Translational Insights
https://www.sciltp.com/journals/ti

Article

A Humanized HLA-Matched Avatar Model for Preclinical Evaluation of DNA Cancer Vaccines

Erika Salvatori [1], Lucia Lione [1], Melanie Paccagnella [1], Eleonora Pinto [1], Mariantonina Greco [1], Emanuele Marra [1], Giuseppe Roscilli [1], Gennaro Ciliberto [1], Luigi Aurisicchio [1,2] and Antonella Conforti [1,2,*]

[1] Takis Biotech, Via Castel Romano 100, 00128 Rome, Italy
[2] Evvivax Biotech, Via Castel Romano 100, 00128 Rome, Italy
* Correspondence: conforti@takisbiotech.it

How To Cite: Salvatori, E.; Lione, L.; Paccagnella, M.; et al. A Humanized HLA-Matched Avatar Model for Preclinical Evaluation of DNA Cancer Vaccines. *Translational Insights* **2026**, *1*(1), 22. https://doi.org/10.53941/ti.2026.100022

Received: 5 June 2026
Revised: 29 July 2026
Accepted: 3 August 2026
Published: 23 September 2026

Abstract: Building on seminal studies which utilized RAG2-deficient mice engrafted with human tumors and reconstituted with human PBMCs to investigate antitumor immunity, the field still lacks robust preclinical systems that faithfully recapitulate human HLA-restricted T cell responses. Here, we describe a humanized murine platform—the HLA-matched Immuno-avatar model—engineered to evaluate DNA-based cancer vaccines delivered by electroporation. The model is based on the adoptive transfer of splenocytes from immunocompetent, vaccinated HLA-A0201 transgenic (HHK) donors into immunodeficient RAG2$^{-/-}$ IL-2Rγ$^{-/-}$ recipients, which are subsequently xenografted with a human colon carcinoma cell line and treated with a DNA vaccine encoding HLA-restricted epitopes of carcinoembryonic antigen (CEA). Transfer of splenocytes from CEA-vaccinated donors induced a robust and statistically significant antitumor effect in recipient mice. This humanized, HLA-matched, and functionally immunocompetent platform provides a flexible and translationally relevant system for the preclinical evaluation of both off-the-shelf and personalized cancer vaccines targeting evolving tumor antigen repertoires.

Keywords: HLA; DNA vaccines; immuno-avatar

1. Introduction

Cancer is a highly heterogeneous and multifactorial disease. Major challenges in the development of effective anticancer therapies include intrinsic and acquired treatment resistance, tumor plasticity and heterogeneity, the presence of a complex and immunosuppressive tumor microenvironment (TME), severe off-target toxicities, and the high economic burden that limits patient access to innovative treatments [1,2]. The design of novel therapeutic strategies must therefore account for tumor-specific molecular features and the dynamic interactions between cancer cells and the TME. In this context, in vivo models remain essential for evaluating antitumor efficacy and immune-mediated mechanisms.

Rodent models have historically provided fundamental insights into tumor biology and treatment responses. However, the translation of preclinical findings to humans remains challenging due to interspecies differences in immunity, metabolism, and tumor evolution [3]. The development of transgenic immunodeficient mouse strains has enabled the engraftment of human tumors and the testing of anticancer drugs. While these xenograft models are suitable for evaluating chemotherapy and targeted therapies, they lack a functional human immune system and therefore cannot recapitulate immune–tumor interactions, which are now recognized as central to tumorigenesis and therapeutic response [4,5]. This underscores the need for more clinically relevant and immunocompetent mouse models.

The advent of immunotherapy with Immune Checkpoint Inhibitors (ICI) has revolutionized cancer treatment by harnessing and amplifying endogenous antitumor immunity. As a result, there is growing interest in identifying optimal murine models for preclinical testing of immunotherapeutics. "Immuno-avatar" models—generated by xenografting patient-derived tumors together with autologous peripheral blood mononuclear cells (PBMCs)—represent a promising platform to reproduce patient specific immune–tumor interactions and to evaluate immunotherapies such as monoclonal antibodies or cancer vaccines alone or in combination with other agents [6–8]. However, their use is limited by the rapid onset of xenograft versus host disease (xeno-GvHD), typically occurring within 3–4 weeks after PBMC transfer, and by the scarcity of PBMCs from vaccinated patients—particularly relevant for the study of neoantigen-based personalized cancer vaccines (PCVs).

PCVs have gained increasing attention as an approach capable of inducing highly specific T cell responses [9,10]. Developing immuno-avatar models suitable for studying such vaccines is highly desirable yet technically challenging. To overcome the limitations of PBMC-based systems, we focused on the preliminary characterization of a translationally relevant murine immuno-avatar model in which vaccine-induced immune and antitumor responses can be evaluated in human tumor xenografts without the confounding effects of early GvHD. The purpose of this research was to verify whether a CD8 immune response against HLA-A0201-restricted neoepitopes is efficacious against human tumors xenografted in immunodeficient RAG2$^{-/-}$ IL2Rγ$^{-/-}$ treated with passive transfer of splenocytes from vaccinated transgenic HHK donors expressing a recombinant version of human HLA-A0201. Although the immune cells used in this system are murine so that the model does not constitute a fully humanized mouse in the classical sense, our scope is to provide a robust and HLA-guided preclinical platform that complements, rather than replaces, conventional humanized mouse approaches.

As an initial step to establish and validate the model, we assessed the well characterized immune and antitumor responses elicited by vaccination against Carcinoembryonic Antigen (CEA). CEA targeting DNA vaccines are known to induce robust T cell responses and tumor protection in C57Bl/6 mice, particularly when delivered by electroporation [11–17]. We first established, as a proof of concept, that CEA-based data can be translated in immuno-avatars challenged with a tumor cell line and subsequently reconstituted with immune cells that are either murine (MC38-CEA and C57Bl/6 splenocytes) or human/humanized, respectively (HCT116 and HHK splenocytes). We therefore evaluated: (i) the viability, localization, and long-term engraftment potential of transferred splenocytes; (ii) the persistence of vaccine-induced immune responses in recipient mice; (iii) the impact on tumor growth in xenografted models.

2. Materials and Methods

2.1. Mice

C57Bl/6 and RAG2$^{-/-}$ IL2Rγ$^{-/-}$ female mice were purchased from Envigo (San Pietro al Natisone, UD, Italy) and used between six and seven weeks of age. Animal experiments were conducted according to Directive 2010/63/EU on the protection of animals used for scientific purposes and implemented in Italy through Legislative Decree no. 26/2014.

2.2. Plasmid Construct and Preparation

Plasmid pV1J/CEAopt carries the codon-usage optimized cDNA of CEA as described [18]. The construct carrying the CEA-LTB fusion was generated by fusing the CEA cDNA from nt 1 to 2037, corresponding to aa 1 to 679, with the LTB cDNA fragment from nt 64 to 375, corresponding to aa 22 to 125. The LTB coding sequence was obtained by PCR amplification of *E. coli* genomic DNA using sequence-specific primers LTB-S1 and LTB-A1. The amplified DNA was introduced at the 3′ end of the CEA coding sequence generating plasmid pV1J/CEAopt-LTB. 50 ng of the plasmid were used to transform 50 µL of competent DH5-alpha *E. coli* cells. Cells were incubated for 30 min on ice, heat-shocked at 42 °C for 30 s and grown for 1 h at 37 °C in Luria-Bertani (LB) medium, in agitation. Cells were then plated on an agar plate containing the selection antibiotic (ampicillin) and incubated overnight at 37 °C. A single bacterial spot expressing resistance to the selection antibiotiCEAc was then picked and grown in LB medium overnight at 37 °C, in agitation. The plasmid was purified using a Giga Prep kit (Thermo Fisher Scientific, Waltham, MA, USA).

2.3. Mice Immunization

Four C57Bl/6 mice were subjected to four weekly DNA injections (50 µg/injection) in a volume of 50 µl in the quadriceps muscle followed by electrical stimulation. Four HHK mice (background C57Bl/6) received one DNA injection (50 µg/injection) in a volume of 50 µL in the quadriceps muscle once a week for four weeks and

followed by electrical stimulation. One week after the last injection, cell-mediated immune response was analyzed. All studies have been performed in accordance with the "Directive 2010/63/EU on the protection of Animals used for scientific purposes" and all the experimental procedures were approved by Takis animal ethical committee and the ethical committee of the Italian Ministry of Health, authorization #A69A0.N.4OC released on 17 May 2023.

2.4. Electroporation

Steel electrodes in the form of parallel 0.2-mm wires about 3 cm long and 5 mm apart were brought into contact with the muscle in parallel orientation with respect to the muscle fibers. The electric field was applied in a pulsed form through an IGEA 5 Cliniporator (Carpi, Italy), and each cycle of stimulation comprised of 8 pulses at 20 ms each at 110 V, 8 Hz, 105 ms intervals.

2.5. Retro-Orbital Blood Collection

Blood samples were collected from the retro-orbital venous plexus under inhalation anesthesia with isoflurane (2–5%). Following anesthesia, mice were gently restrained to induce exophthalmos, and blood was collected using a sterile glass Pasteur pipette inserted into the medial canthus of the lower eyelid. Gentle pressure and rotation of the pipette enabled blood collection by capillary action, followed by transfer into collection tubes. Blood volumes ranging from 100 to 400 µL were obtained depending on mice age and body weight. Whole blood samples were lysed with ACK lysis buffer (Thermo Fisher Scientific, Waltham, MA, USA), washed with RPMI medium supplemented with 10% fetal bovine serum (FBS, Thermo Fisher Scientific, Waltham, MA, USA), and resuspended in the same medium for subsequent stimulation and staining analyses.

2.6. Peritoneal Lavage

Peritoneal lavage was performed immediately after euthanasia. Mice were placed in a supine position, and the abdominal surface was disinfected with 70% ethanol. The outer abdominal skin was carefully reflected to expose the intact peritoneal wall. Five milliliters of ice-cold PBS were injected into the peritoneal cavity using a 27-gauge needle. The abdomen was gently massaged for 30–60 s to detach peritoneal cells, and the lavage fluid was recovered using a 5-mL syringe fitted with a 25-gauge needle. Lavage fluid was kept on ice, centrifuged at 400× *g* for 8 min at 4 °C, and the cell pellet was resuspended in PBS or appropriate medium for cell counting and subsequent analyses.

2.7. Cell Lines

MC38-CEA is a murine colon carcinoma of C57Bl/6 origin purchased from ATCC (Manassas, VA, USA) and stably transfected to express human carcinoembryonic antigen (CEA). Cells were cultured in Dulbecco's Modified Eagle Medium (Thermo Fisher Scientific, Waltham, MA, USA), supplemented with 10% heat-inactivated fetal bovine serum, 1% penicillin/streptomycin and 1% glutamine, at 37 °C and 5% CO_2. G418 (Merck, Darmstadt, Germany) was added to the cell medium at a final concentration of 400 µg/mL to select CEA-expressing MC38.

HCT116 is a human colon carcinoma cell line purchased from ATCC and cultured in Dulbecco's Modified Eagle Medium (Thermo Fisher Scientific, Waltham, MA, USA), supplemented with 10% heat-inactivated fetal bovine serum [nome ditta, Thermo Fisher Scientific, Waltham, MA, USA], 1% penicillin/streptomycin and 1% glutamine. HCT116 cells were also tested for the expression of both CEA and HLA-A2 on a CytoFLEX flow cytometer (Beckman Coulter, Brea, CA, USA) using anti-CEA and anti-human HLA-A0201-PE-Cy7 conjugated antibody (eBioscience, San Diego, CA, USA).

2.8. Tumor Challenge Studies

Six RAG2$^{-/-}$ IL2Rγ $^{-/-}$ mice were challenged each with a subcutaneous injection of 2×10^5 MC38-CEA suspended in 100 µL PBS (Phosphate Buffered Saline) in the right flank. Twelve RAG2$^{-/-}$ IL2Rγ$^{-/-}$ mice were challenged each with a subcutaneous injection of 5×10^6 HCT116 suspended in a volume of 100 µL PBS. Twice a week, mice were examined for tumor growth using a caliper. Tumor volumes were calculated using the formula: length × width^2 × 0.5.

2.9. Adoptive Transfer Studies

Splenocytes from either vaccinated or naive C57Bl/6 mice were lysed in ACK lysing buffer, washed twice in PBS, pooled together and injected in the peritoneum of the RAG2$^{-/-}$ IL2Rγ $^{-/-}$mice recipients when the MC38-

CEA tumors reached 200–300 mm^3. Each recipient received 15×10^6 splenocytes in a volume of 100 µL PBS. The same amount of splenocytes was also inoculated in 12 mice without the tumors, with the purpose to verify cell viability and the persistence of the immune response.

2.10. Peptides

Lyophilized CEA peptides were purchased from JPT (Amsterdam, NL) and resuspended in dimethyl sulphoxide (DMSO) at 40 mg/mL. A pool of 4 distinct peptides 15 amino acids long overlapping by 11 residues was assembled and the final concentration of each peptide in the pool was 0.2 mg/mL.

2.11. Cytokine Intracellular Staining

Mouse PBMCs or splenocytes were incubated for 10 min at room temperature in ACK (Ammonium-Chloride-Potassium) Lysing Buffer, which is used for the lysis of red blood cells in samples containing white blood cells, and then washed in RPMI-10% fetal bovine serum (FBS). 1–2 million mouse PBMCs or splenocytes were resuspended in RPMI-10% FBS and transferred to a 96-well plate and incubated with the indicated pool of peptides in a 1:1 cells/peptide pool ratio (the final concentration of each peptide in the well was 0.1 mg/mL) and Brefeldin A (1 µg/mL; BD) at 37 °C for 12–16 h. DMSO and PMA-ionomycin were used as negative and positive controls, respectively. Cells were then washed twice in PBS and dead cells were stained using Live/Dead Fixable Yellow dead cell stain kit (Thermo Fisher Scientific, Waltham, MA, USA) for 20 min at room temperature. Cells were washed twice with PBS-0.5% bovine serum albumin (BSA) and incubated with a mouse Fc receptor blocker (anti-CD16/CD32; eBioscience) for 15 min at 4 °C. Cells were washed twice with PBS-0.5% BSA and stained with conjugated surface antibodies anti-CD3-FITC, anti-CD4-PerCP-Cy5.5 and CD8-APC-eFluor780 (eBioscience, San Diego, CA, USA), for 25–30 min at 4 °C. Cells were washed and fixed in IC Fixation buffer (eBioscience) for 20 min at 4 °C, permeabilized (permeabilization buffer, eBioscience) and incubated with conjugated intracellular antibodies anti-IFN-γ-PE, TNF-α-PE-Cy7 and IL-2-APC (eBioscience) for 25–30 min at 4 °C. Finally, cells were washed, resuspended in PBS and analyze on a CytoFLEX flow cytometer (Beckman Coulter). Analysis was performed using CytExpert software v2.6 (Beckman Coulter).

2.12. Statistical Analyses

Statistical analyses were performed using GraphPad Prism version 8.0.2. Survival curves were analyzed using the log-rank (Mantel–Cox) test. Comparisons between two independent groups were performed using the Mann–Whitney U test. Data are presented as mean ± SEM unless otherwise specified. A p-value < 0.05 was considered statistically significant (*).

3. Results

3.1. Assessment of CEA-Specific Cellular Immune Response in C57Bl/6 Donors

We first characterized a fully murine model of immuno-avatar where splenocytes from four C57Bl/6 vaccinated donors were transplanted in $RAG2^{-/-}$ $IL2R\gamma^{-/-}$ recipients. To this aim, four C57Bl/6 mice were vaccinated with a protocol consisting of four weekly injections of plasmid pVIJ/CEAopt-LTB - a DNA vector encoding for CEA fused to Heat Labile Toxin B (LTB) from *E. Coli* or the empty vector by electroporation (DNA-EP). One week after the last immunization, mice were culled and the CEA-specific cellular immune response was measured by IFN-γ, TNF-α and IL-2 intracellular cytokine staining (ICS) performed on both splenocytes and PBMCs using a pool of immunodominant CEA-peptides selected in previous papers as stimulus [18]. As expected, no CEA specific immune response was measured in naïve C57Bl/6 derived cells, whereas both $CD8^+$ and $CD4^+$ specific immune responses were revealed only in the samples collected from the mice vaccinated with the CEA encoding vector (Figure 1). The vaccination predominantly induced a $CD8^+$ T cell specific immune response, which was particularly evident in peripheral blood, where an increased frequency of circulating $CD8^+$ T cells producing IFN-γ was observed.

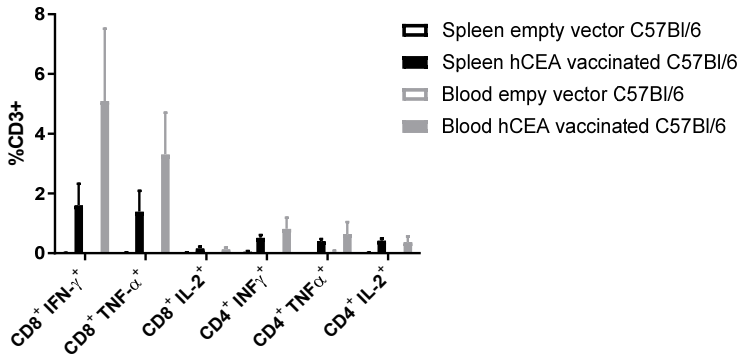

Figure 1. Assessment of CEA-specific immune response by means of intracellular cytokine staining on splenocytes and PBMCs isolated from both naïve and CEA-vaccinated C57Bl/6. Statistical analysis was performed by comparing splenocytes or PBMCs derived from CEA-vaccinated mice with those derived from mice vaccinated with the empty vector control. Data are presented as mean ± SEM.

3.2. Persistence of Adoptively Transferred C57Bl/6 Splenocytes in RAG2$^{-/-}$ IL2Rγ$^{-/-}$ Recipient Mice

Once the ability of pVIJ/CEAopt-LTB vaccine delivered by DNA-EP to induce a strong immune response in the donors was assessed, splenocytes of either vaccinated or control group mice were injected intraperitoneally in six RAG2$^{-/-}$ IL2Rγ$^{-/-}$ recipients per group. In order to assess the viability of the injected splenocytes, CD3$^+$, CD4$^+$ and CD8$^+$ T cells were measured by flow cytometry in the blood of the recipient mice one and three weeks after transplantation. The results show the successful engraftment of the adoptively transferred splenocytes, but at the same time, a progressive reduction of the CD4$^+$/CD8$^+$ ratio in the blood (Figure 2A,B). In fact, at the three weeks' time point from splenocytes transplantation, the percentage of CD4$^+$ T cells in the blood was minimal. To further investigate the distribution of the transplanted splenocytes, and in particular of the CD4$^+$ T cells, two recipient mice were sacrificed at five weeks from splenocytes transplantation, and CD45$^+$, CD3$^+$, CD4$^+$ and CD8$^+$ T cells were measured in both blood and splenocytes. The analysis performed on PBMCs confirmed the progressive loss of CD4$^+$ T cells in the peripheral blood, whereas a robust CD4$^+$ T cells population was found to be resident in the spleen (Figure 2B,C).

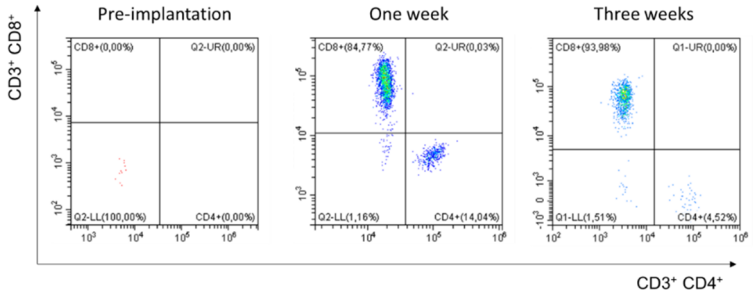

(**A**)

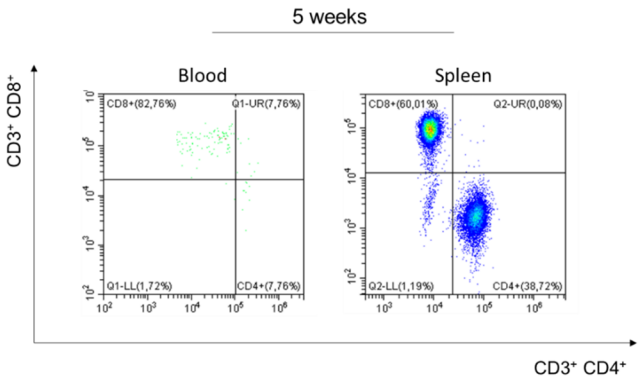

(**B**)

Figure 2. *Cont.*

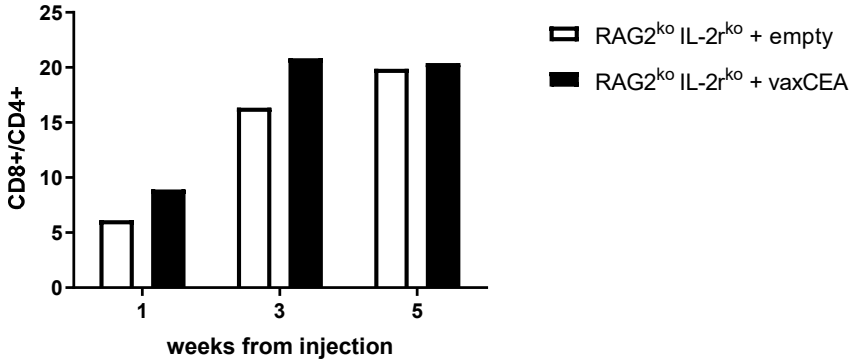

(**C**)

Figure 2. (**A**) Peripheral blood from one representative recipient mouse was analyzed by flow cytometry at 1 and 3 weeks post-transplantation using CD3, CD4, and CD8 staining to evaluate the persistence of donor splenocytes. (**B**) A surface staining performed at 5 weeks from splenocytes transplantation on both blood and spleen showed that CD4+ T cells were resident in the spleen of recipient mice. (**C**) A progressive increase of the $CD8^+/CD4^+$ ratio was observed in the blood of the recipients.

3.3. RAG2$^{-/-}$ IL2Rγ$^{-/-}$ Recipient Mice Show Measurable CEA-Specific CD8$^+$ Immune Responses

To evaluate the persistence of the immune response against CEA in RAG2$^{-/-}$ IL2Rγ$^{-/-}$ recipients, an intracellular staining for the cytokines IFN-γ, TNF-α, and IL-2 was performed one and three weeks after splenocytes transplantation on PBMCs restimulated with a pool of immunodominant CEA peptides (Figure 3). $CD3^+$ $CD8^+$ T cells producing IFN-γ were significantly increased in the mice that received splenocytes from vaccinated donors as compared with the control after one week from splenocytes transplantation. Nonetheless, IFN-γ- producing cells decreased over time and were no longer present in significant amounts in the blood circulation after three weeks from splenocytes transplantation.

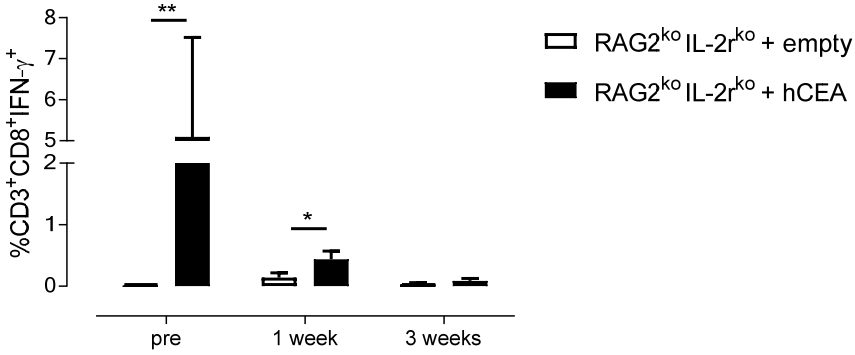

Figure 3. The intracellular cytokine staining was performed at 1 and 3 weeks from splenocytes transplantation to verify the persistence of the CEA-specific immune response in the blood of recipients. IFN-γ producing $CD8^+$ T cells were significantly increased in the recipient mice after 1 week from splenocytes transplantation, but their concentration decreased over time becoming negligible after 3 weeks. Mann-Whitney U test was used for two groups comparison. Data are presented as mean ± SEM. The * indicates a p-value < 0.05. The ** indicate a p-value < 0.001.

3.4. Antitumoral Effect of Adoptively Transferred CEAopt-LTB-Vaccinated Splenocytes from C57Bl/6 Donors in RAG2$^{-/-}$ IL2Rγ$^{-/-}$ Recipients

To assess the antitumoral effect of pVIJ/CEAopt-LTB vaccination in transplanted recipients in a therapeutic setting, six RAG2$^{-/-}$ IL2Rγ$^{-/-}$ mice were injected subcutaneously with 2×10^5 MC38-CEA, a syngeneic tumor cell line that expresses CEA, and subsequently treated with splenocytes from either vaccinated or naïve C57Bl/6 donors at day 21, when the MC38-CEA tumors reached 200–300 mm^3. Tumor growth was monitored for 60 days and results are reported in Figure 4. We observed a significant delay in tumor growth in the mice engrafted with splenocytes from the CEA-vaccinated donors, with a partial regression observed in only one mouse (Figure 4A).

Importantly, the transplantation of splenocytes from CEA-vaccinated donors significantly increased the survival of the recipients as compared with the control group (Figure 4B).

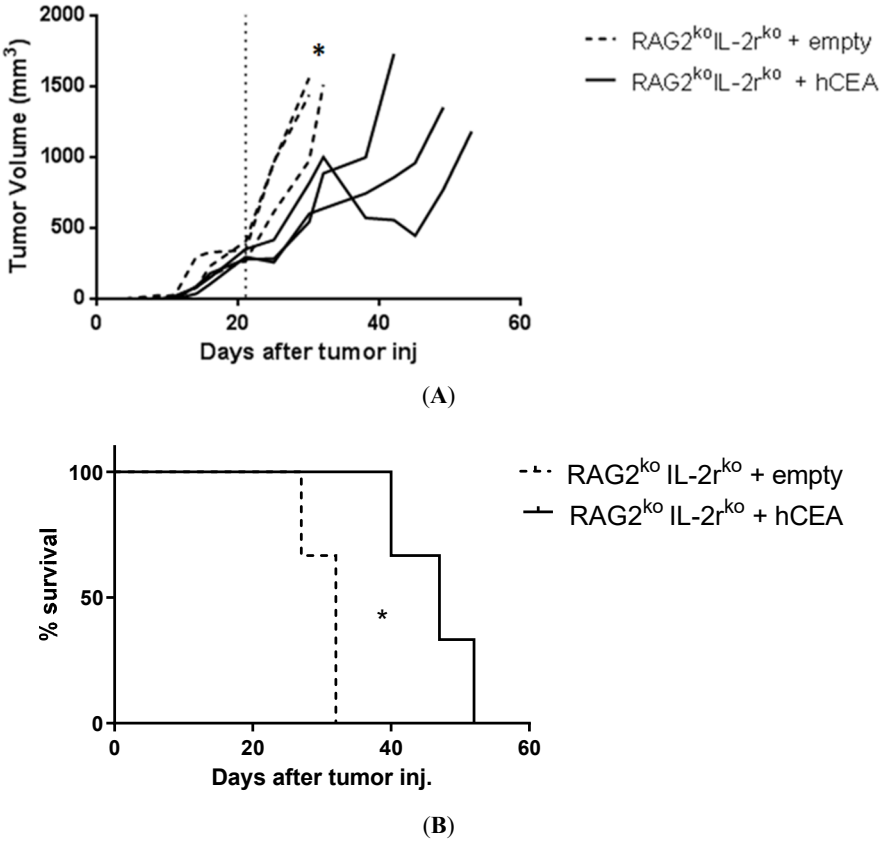

Figure 4. (**A**) The antitumoral response was evaluated in a therapeutic setting on 6 RAG2$^{-/-}$ IL2Rγ$^{-/-}$ that were inoculated with 2 × 10^5 MC38-CEA and subsequently treated at day 21 (vertical dashed line) with splenocytes from either vaccinated or naïve C57Bl/6 donors: (*p*-value: 0.027). (**B**) The transplantation of splenocytes from vaccinated donors significantly increased the survival of the recipients as compared with control group (*p*-value: 0.0224). Tumor growth delay was calculated by comparing the mean tumor volume values between the two experimental groups at the end of the observation period using the Mann–Whitney U test. The humane endpoint was defined as a tumor volume of 1500 mm^3, at which mice were euthanized according to the experimental protocol. Survival curves were analyzed using the log-rank (Mantel–Cox) test. The * indicates a *p*-value <0.05.

3.5. Evaluation of CEA- and LTB-Specific Immune Response in HHK Donors

The previously characterized model was progressively translated from a fully murine model to a humanized system. This was accomplished using HHK transgenic mice that express human HLA-A0201 as splenocyte donors. Four HHK mice were vaccinated with a protocol consisting of four weekly DNA-EP injection of the plasmid pVIJ/CEAopt-LTB or the empty vector. One week after the last immunization, the immune response was measured by IFN-γ and TNF-α intracellular staining on PBMCs restimulated with a pool of immunodominant CEA-peptides. A detectable CEA-specific CD4$^+$ immune response was measured, whereas CEA-specific CD8$^+$ immune response was lower. Since the estimated percentage of CD8$^+$ T cells measured in HHK transgenic mice is approximately 1/5 lower than what was observed in wild type C57Bl/6, it is unlikely to measure significant CD8$^+$ T cell responses from peripheral blood. In order to confirm that immunization had occurred, we performed a second intracellular cytokine staining on PBMCs restimulated with either a pool of CEA peptides or LTB-derived peptides, showing a statistically significant response to LTB peptides from both CD8$^+$ and CD4$^+$ cells (Figure 5A). A comparable response, but only from CD4$^+$ cells, was also observed on the splenocytes (Figure 5B). After one week from splenocytes transplantation, a surface staining on spleen, blood and peritoneal lavage of RAG2$^{-/-}$ IL2Rγ$^{-/-}$ recipients showed the presence of transplanted splenocytes, especially in the spleen and in the peritoneal lavage (Figure 5C).

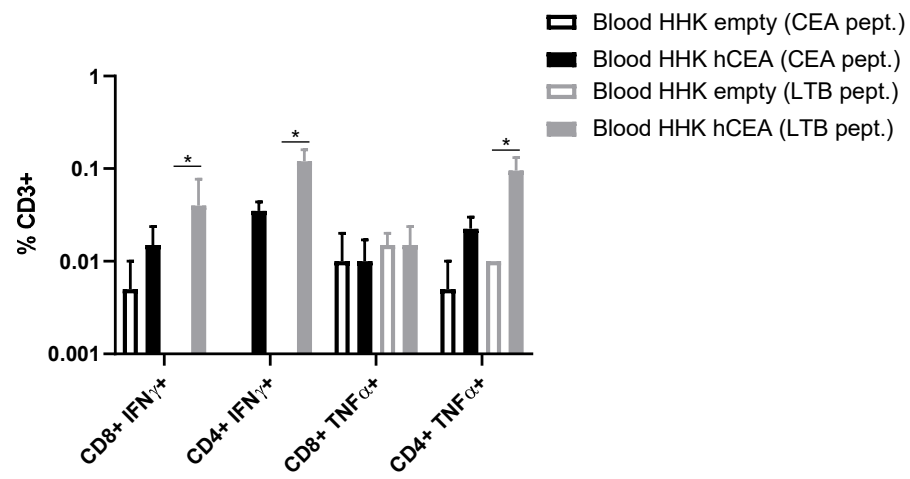

(**A**)

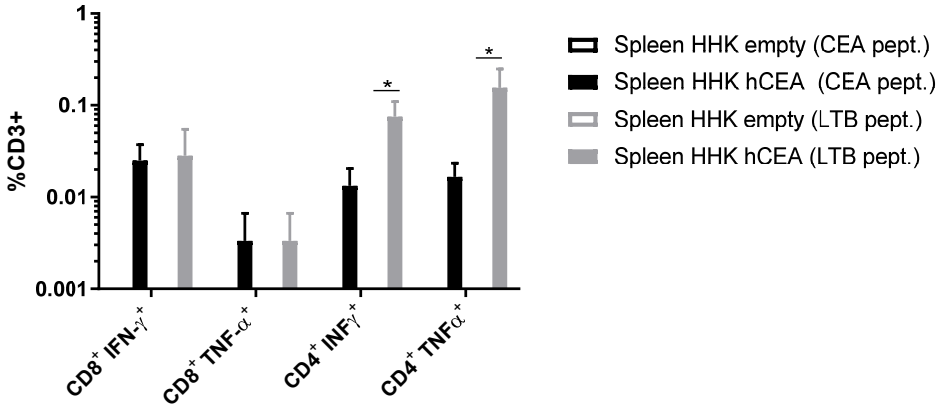

(**B**)

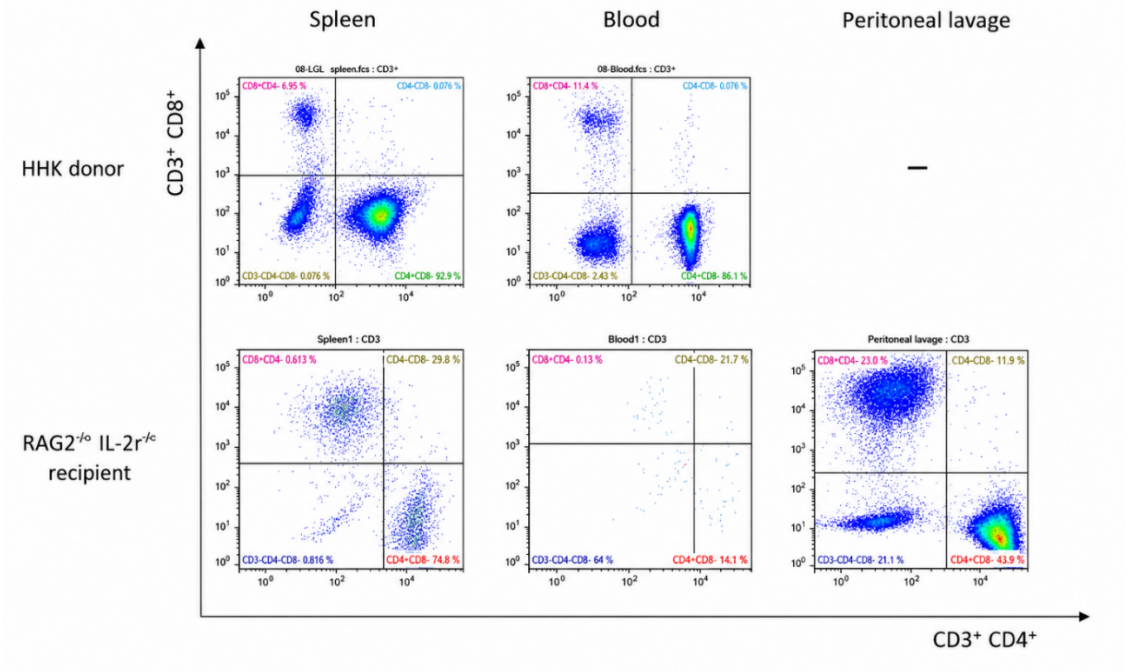

(**C**)

Figure 5. (**A**,**B**) $CD8^+$ specific immune response was not as high as expected, particularly upon stimulation with CEA peptides; nevertheless, $CD4^+$ specific responses were measured in a statistically significant measure upon stimulation with both CEA and LTB peptides, in blood as well in spleen. (*p*-value 0.0286; 0.0245). The * indicates a *p*-value < 0.05. (**C**) Surface staining on spleen, blood and peritoneal lavage of $RAG2^{-/-}$ $IL2R\gamma^{-/-}$ recipients showing the presence of transplanted splenocytes.

3.6. Anti-Tumor Effect of Adoptively Transferred CEAopt-LTB-Vaccinated Splenocytes from HHK Donors in RAG2$^{-/-}$ IL2Rγ$^{-/-}$ Recipients

Once it was assessed that vaccination had elicited a detectable antigen-specific immune response, the mice were culled and the splenocytes were injected intraperitoneally in RAG2$^{-/-}$ IL2Rγ$^{-/-}$ recipients. The scarce amount of CD8^{+} T cells in the HHK donors was taken into consideration when calculating the amount of splenocytes necessary for transplantation. Together with the splenocytes transplantation, the recipients were also challenged subcutaneously with 5×10^6 HCT116, a human colon carcinoma cell line which had been tested for the expression of both CEA and HLA-A0201. Tumor growth was monitored to establish whether adoptively transferred splenocytes from vaccinated donors were able to impair the progression of a human tumor cell line. Palpable, not measurable, tumor masses were observed only in the control group. As a consequence, in order to investigate the presence of internal masses, mice were sacrificed for a visual inspection. 4 out of 4 mice in the control group that had received no splenocytes transplantation developed detectable tumor masses; only 2 out of 4 mice in the group that had received naïve splenocytes transplantation developed tumor masses; no mouse in the group that had received vaccinated splenocytes developed tumors (Figure 6). The experiment was independently replicated with the same number of mice, yielding comparable results.

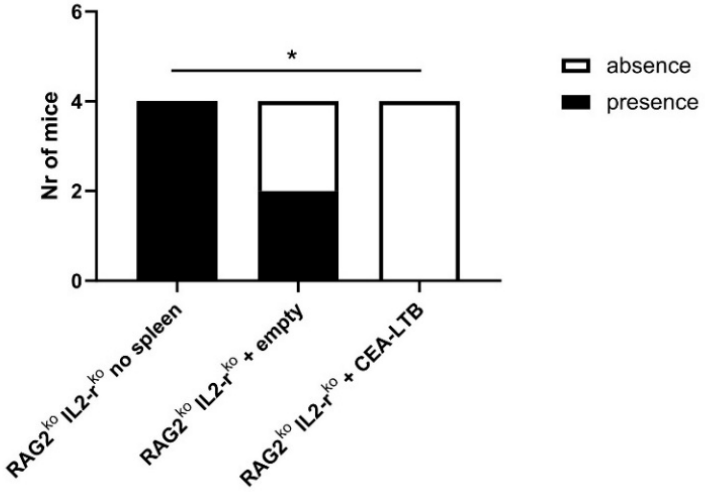

Figure 6. At cull (20 days post transplantation), all the mice in the control group without splenocyte transplantation had developed the tumor. In the group that had received splenocytes from naïve HHK, only 2 out of 4 mice had developed a tumor mass although not measurable. In the group that had received splenocytes from CEA-LTB vaccinated HHK mice, all the mice were tumor-free (*p-value*: 0.011). Four animals per group were included in this experiment. The * indicates a *p*-value <0.05.

4. Discussion

This study aimed to generate and characterize a murine immuno-avatar model suitable for evaluating the efficacy of genetic cancer vaccines against human tumors in preclinical settings. Our strategy is based on the adoptive transfer of splenocytes from immunocompetent, vaccinated HLA-A0201 transgenic donors (HHK mice) into immunodeficient RAG2$^{-/-}$ IL2Rγ$^{-/-}$ recipients, which can subsequently be xenografted with HLA-matched human tumors. This approach addresses the limitations of conventional xenograft models, which lack a functional human immune system, and of PBMC-based immuno-avatars, which are constrained by limited cell availability and rapid onset of xenograft-versus-host disease (xeno-GvHD) [19–21].

To assess feasibility, we first performed a proof-of-concept study with a mouse-only immuno-avatar model using splenocytes from CEA-vaccinated C57Bl/6 donors transplanted into strongly immunodeficient RAG2$^{-/-}$ IL2Rγ$^{-/-}$ mice. This allowed us to evaluate (i) the viability and persistence of transferred splenocytes, (ii) the durability of vaccine-induced immune responses, and (iii) the antitumor activity in a therapeutic setting. Once this approach was established, we translated it to a humanized context testing, in which splenocytes from CEA-vaccinated HHK donors were passively transferred into RAG2$^{-/-}$ IL2Rγ$^{-/-}$ mice xenografted with HLA-matched human tumor cells. Transferred splenocytes remained viable for at least five weeks, indicating that the RAG2$^{-/-}$ IL2Rγ$^{-/-}$ environment supports short-term immune cell engraftment, consistent with previous observations in lymphopenic hosts [22,23]. However, CD4^{+} T cells rapidly disappeared from peripheral blood despite being

detectable in the spleen. This phenomenon aligns with evidence showing that IL-2 signaling is essential for $CD4^+$ T cell proliferation, survival, and homeostasis [24,25]. The absence of IL-2 receptor activity in the host likely skews the $CD4^+/CD8^+$ ratio and selectively impairs $CD4^+$ T-cell maintenance in circulation. Similar imbalances have been reported in other IL2Rγ-deficient models [26]. Additional characterization of the transferred immune cells—particularly their persistence and functional activity within the tumor microenvironment—would further reinforce the biological relevance and translational potential of the model.

The magnitude of the vaccine-induced immune response in immuno-avatar mice was significantly lower than in donor mice. Although still detectable one week after splenocytes transfer, the response declined rapidly, as expected in an HLA-I-restricted model, where the frequency of antigen-specific $CD8^+$ T cells is inherently reduced compared to fully primed donors. This suggests that either the priming strategy or the adoptive transfer procedure requires optimization. For example, enrichment of $CD4^+$ or $CD8^+$ T cell subsets prior to transfer may increase the frequency of antigen-specific cells and improve detectability, as demonstrated in adoptive T cell therapy studies [27,28]. Additional strategies could further potentiate immune activation, such as the co-injection of plasmids encoding immunostimulatory cytokines—e.g., IL-17, IL-12, or IL-15—which have been shown to enhance T-cell priming, effector differentiation, and antitumor activity [29–31]. Likewise, incorporating STING agonists or vectors expressing STING-activating molecules could amplify type I interferon signaling and strengthen the innate–adaptive interface, thereby improving the overall magnitude and durability of vaccine-elicited responses [32,33].

The evaluation of antitumor activity revealed context-dependent outcomes. In a therapeutic setting, splenocytes transfer significantly delayed tumor growth in mice bearing MC38-CEA tumors, and in some cases induced complete tumor regression. Although tumor progression eventually resumed—likely due to the waning of passive immunity—the overall survival of treated mice was significantly improved. These findings indicate that transferred immune cells retain functional antitumor activity, consistent with previous reports showing that vaccine-primed T cells can mediate tumor control even in partially supportive environments [10,34]. Consistent with our previously published findings, preliminary experiments performed using the humanized immuno-avatar model showed that transferring splenocytes from HHK-vaccinated donors blocks melanoma M285 growth and induces tumor regression in U11 lung cancer xenografts, but in the present work we evaluate a shared tumor-associated antigen (CEA), thereby extending the model beyond personalized neoepitope settings and demonstrating its broader translational utility [35]. Although no statistically significant differences in tumor growth were observed between mice receiving splenocytes from vaccinated versus naïve donors, post-mortem inspection revealed that 50% of mice receiving naïve splenocytes developed small internal tumor masses, whereas all mice receiving splenocytes from vaccinated donors were tumor-free. This observation, although limited to a small number of mice, suggests a potential contribution of vaccine-primed splenocytes to tumor control, while acknowledging that the experiment is underpowered and that complete regression was not consistently observed. This also indicates that naïve splenocytes may exert nonspecific early antitumor effects—possibly through innate-like lymphocytes or homeostatic proliferation—but only vaccine-primed splenocytes can prevent tumor establishment when the tumor burden remains below a critical threshold [36]. Moreover, validating this finding in an independent tumor model expressing a different antigen would strengthen this conclusion, and further confirmatory studies are warranted.

Overall, our findings support the feasibility of using splenocytes-based immuno-avatars to evaluate vaccine-induced immune and antitumor responses in a humanized context. However, the model requires further optimization to enhance the durability and magnitude of immune responses, particularly for weakly immunogenic antigens such as neoepitopes. Future improvements may include cytokine supplementation (e.g., IL-7 or IL-15), co-transfer of antigen-presenting cells, or engineering of the host environment to better support humanized immune cell function [37,38]. These refinements could significantly increase the translational relevance of the model for preclinical testing of next-generation cancer vaccines.

5. Conclusions

Immunotherapy has emerged as a powerful strategy for cancer treatment; however, its rapid evolution has also exposed the limitations of conventional animal models. Building on the concept of immuno-avatar systems developed to study immune-checkpoint inhibitors and their combinations with other immunotherapies, we proposed a new translational platform enabling the validation of HLA-A0201–restricted cancer vaccines on human HLA-matched tumor xenografts. Our study demonstrates, for the first time, that this approach is feasible and capable of fulfilling its intended purpose, although several limitations remain and substantial opportunities for refinement exist. In this regard, this model could also be leveraged in the future to investigate the dynamic interactions between immune cells and tumor cells within the microenvironment through spatial microscopy.

In perspective, within the expanding field of precision medicine, we believe that personalized genetic vaccines targeting predicted neoepitopes represent a promising therapeutic avenue. Together, neoepitope vaccines and immuno-avatar models are paving the way toward a personalized oncology framework in which each patient may receive therapies tailored to their individual tumor and immune profile, and whose safety and efficacy can be pre-clinically evaluated in animal models faithfully reproducing the specific interaction between the patient's tumor and immune system. This model can be further optimized. Patient-derived PBMCs could be collected, primed in vitro with the antigen of interest, and subsequently transferred into immunodeficient recipients bearing patient-derived xenografts to assess vaccine efficacy. Alternatively, PBMCs from vaccinated patients enrolled in clinical trials could be engrafted into immuno-avatars to investigate potential combinatorial strategies, including immune-checkpoint blockade or chemotherapeutic agents.

Author Contributions

E.S., L.L., M.P., E.P. and M.G. performed experiments; E.S., L.A. and A.C. analyzed and interpreted data; E.S. and A.C. prepared the figures; E.M., G.R., G.C., L.A. and A.C. provided conceptual advice and edited the manuscript. All authors have read and agreed to the published version of the manuscript.

Funding

This work was supported by IPCEI Med For Cure- Progetto Zetesis X-eVax- Sa.105085 CUP B89J25000270005.

Institutional Review Board Statement

The study was conducted according to Takis internal ethical committee guidelines and approved on 17 May 2023 by the ethical committee of the Italian Ministry of Health, authorization A69A0.N.4OC.

Informed Consent Statement

Not applicable.

Data Availability Statement

All data are available in the main text.

Conflicts of Interest

All the authors are currently employees at Evvivax and Takis companies, which are currently developing proprietary nucleic-acid vaccines based on DNA-EP. The authors declare no other conflicts of interest.

Use of AI and AI-Assisted Technologies

No AI tools were utilized for this paper.

References

1. Hanahan, D. Hallmarks of cancer: New dimensions. *Cancer Discov*. **2022**, *12*, 31–46.
2. Havel, J.J.; Chowell, D.; Chan, T.A. The evolving landscape of biomarkers for checkpoint inhibitor immunotherapy. *Nat. Rev. Cancer* **2019**, *19*, 133–150.
3. Day, C.P.; Merlino, G.; Van Dyke, T. Preclinical mouse cancer models: A maze of opportunities and challenges. *Cell* **2015**, *163*, 39–53.
4. Binnewies, M.; Roberts, E.W.; Kersten, K.; et al. Understanding the tumor immune microenvironment (TIME) for effective therapy. *Nat. Med*. **2018**, *24*, 541–550.
5. Joyce, J.A.; Fearon, D.T. T cell exclusion, immune privilege, and the tumor microenvironment. *Science* **2015**, *348*, 74–80.
6. Melero, I.; Sanmamed, M.F.; Chester, C.; et al. Defining the optimal murine models to investigate immune checkpoint blockers and their combination with other immunotherapies. *Ann. Oncol*. **2016**, *27*, 1190–1198.
7. Hidalgo, M.; Amant, F.; Biankin, A.V.; et al. Patient-derived xenograft models: An emerging platform for translational cancer research. *Cancer Discov*. **2014**, *4*, 998–1013.
8. Brandenburg, A.; Heine, A.; Brossart, P. Next-generation cancer vaccines and emerging immunotherapy combinations. *Trends Cancer* **2024**, *10*, 749–769.

9. Ott, P.A.; Hu, Z.; Keskin, D.B.; et al. An immunogenic personal neoantigen vaccine for patients with melanoma. *Nature* **2017**, *547*, 217–221.
10. Sahin, U.; Türeci, Ö. Personalized vaccines for cancer immunotherapy. *Science* **2018**, *359*, 1355–1360.
11. Hance, K.W.; Zeytin, H.E.; Greiner, J.W. Mouse models expressing human carcinoembryonic antigen (CEA) as a transgene: Evaluation of CEA-based cancer vaccines. *Mutat. Res*. **2005**, *576*, 132–154.
12. Gameiro, S.R.; Jammeh, M.L.; Hodge, J.W. Cancer vaccines targeting carcinoembryonic antigen: State-of-the-art and future promise. *Expert Rev. Vaccines* **2013**, *12*, 617–629.
13. Conforti, A.; Peruzzi, D.; Giannetti, P.; et al. A novel mouse model for evaluation and prediction of HLA-A2-restricted CEA cancer vaccine responses. *J. Immunother*. **2009**, *32*, 744–754.
14. Turriziani, M.; Fantini, M.; Benvenuto, M.; et al. Carcinoembryonic antigen (CEA)-based cancer vaccines: Recent patents and antitumor effects from experimental models to clinical trials. *Recent Pat Anticancer. Drug Discov*. **2012**, *7*, 265–296.
15. Facciabene, A.; Aurisicchio, L.; Elia, L.; et al. Vectors encoding carcinoembryonic antigen fused to the B subunit of heat-labile enterotoxin elicit antigen-specific immune responses and antitumor effects. *Vaccine* **2008**, *26*, 47–58.
16. Aurisicchio, L.; Roscilli, G.; Marra, E.; et al. Superior immunologic and therapeutic efficacy of a xenogeneic genetic cancer vaccine targeting carcinoembryonic antigen. *Hum. Gene Ther*. **2015**, *26*, 386–398.
17. Kisakova, D.N.; Belyakov, I.M.; Kisakova, L.A.; et al. The use of electroporation to deliver DNA-based vaccines. *Expert Rev. Vaccines* **2024**, *23*, 102–123.
18. Mennuni, C.; Calvaruso, F.; Facciabene, A.; et al. Efficient induction of T-cell responses to carcinoembryonic antigen by a heterologous prime-boost regimen using DNA and adenovirus vectors carrying a codon-optimized cDNA. *Int. J. Cancer* **2005**, *117*, 444–455.
19. Rongvaux, A.; Willinger, T.; Takizawa, H.; et al. Human hemato-lymphoid system mice: Current use and future potential for medicine. *Annu. Rev. Immunol.* **2014**, *32*, 563–599.
20. Morton, J.J.; Bird, G.; Refaeli, Y.; et al. Humanized Mouse Xenograft Models: Narrowing the Tumor-Microenvironment Gap. *Cancer Res.* **2016**, *76*, 6153–6158.
21. Walsh, N.C.; Kenney, L.L.; Jangalwe, S.; et al. Humanized mouse models of clinical disease. *Annu. Rev. Pathol*. **2017**, *12*, 187–215.
22. Billerbeck, E.; Barry, W.T.; Mu, K.; et al. Development of human $CD4^+$ T cells in humanized mice. *J. Clin. Investig.* **2011**, *117*, 3076–3086.
23. Shultz, L.D.; Brehm, M.A.; Garcia-Martinez, J.V.; et al. Humanized mice for immune system investigation: Progress, promise and challenges. *Nat. Rev. Immunol*. **2012**, *12*, 786–798.
24. Boyman, O.; Sprent, J. The role of interleukin-2 during homeostasis and activation of the immune system. *Nat. Rev. Immunol*. **2012**, *12*, 180–190.
25. Liao, W.; Lin, J.-X.; Leonard, W.J. Interleukin-2 at the crossroads of effector responses, tolerance, and immunotherapy. *Immunity* **2013**, *38*, 13–25.
26. Alcantar-Orozco EM; Gornall H; Baldan V; et al. Potential limitations of the NSG humanized mouse as a model system to optimize engineered human T cell therapy for cancer. *Hum Gene Ther Methods*. **2013**, *24*, 310–320.
27. Rosenberg, S.A.; Restifo, N.P. Adoptive cell transfer as personalized immunotherapy for human cancer. *Science* **2015**, *348*, 62–68.
28. Krishna, S.; Lowery, F.J.; Copeland, A.R.; et al. Stem-like CD8 T cells mediate response of adoptive cell immunotherapy against human cancer. *Science* **2020**, *370*, 1328–1334.
29. Kryczek, I.; Wei, S.; Szeliga, W.; et al. Endogenous IL-17 contributes to reduced tumor growth and metastasis. *Blood* **2009**, *114*, 357–359.
30. Trinchieri, G. Interleukin-12 and the regulation of innate resistance and adaptive immunity. *Nat. Rev. Immunol*. **2003**, *3*, 133–146.
31. Waldmann, T.A. Interleukin-15 (dys)regulation of lymphoid homeostasis: Implications for therapy of autoimmunity and cancer. *J. Exp. Med*. **2020**, *217*, e20191062.
32. Corrales, L.; Glickman, L.H.; McWhirter, S.M.; et al. Direct activation of STING in the tumor microenvironment leads to potent and systemic tumor regression. *Cell Rep.* **2015**, *11*, 1018–1030.
33. Sivick, K.E.; Desbien, A.L.; Glickman, L.H.; et al. Magnitude of therapeutic STING activation determines $CD8^+$ T-cell–mediated anti-tumor immunity. *J Immunol*. **2017**, *198*, 1579–1590.
34. Melero, I.; Castanon, E.; Alvarez, M.; et al. Intratumoural administration and tumour tissue targeting of cancer immunotherapies. *Nat. Rev. Clin. Oncol.* **2021**, *18*, 558–576.
35. Aurisicchio, L.; Salvatori, E.; Lione, L.; et al. Poly-specific neoantigen-targeted cancer vaccines delay patient derived tumor growth. *J. Exp. Clin. Cancer Res*. **2019**, *38*, 78.
36. Jameson, S.C.; Lee, Y.J.; Hogquist, K.A. Innate memory T cells. *Nat. Rev. Immunol*. **2015**, *15*, 135–145.

37. Sefik, E.; Xiao, T.; Chiorazzi, M.; et al. Engineering Mice to Study Human Immunity. *Annu Rev Immunol*. **2025**, *43*, 451–487.
38. Brehm, M.A.; Kenney, L.L.; Wiles, M.V.; et al. Lack of acute xenogeneic graft-versus-host disease, but retention of T-cell function following engraftment of human peripheral blood mononuclear cells in NSG mice deficient in MHC class I and II expression. *FASEB J*. **2019**, *33*, 3137–3151.